Pulsatile actomyosin contractions underlie Par polarity during the neuroblast polarity cycle

Chet Huan Oon and Kenneth E. Prehoda*

Institute of Molecular Biology
Department of Chemistry and Biochemistry
1229 University of Oregon
Eugene, OR 97403

*Corresponding author: prehoda@uoregon.edu

Abstract

The Par complex is polarized to the apical cortex of asymmetrically dividing *Drosophila* neuroblasts. Previously we showed that Par proteins are polarized by apically directed cortical movements that require F-actin (Oon and Prehoda, 2019). Here we report the discovery of cortical actin pulses that begin before the Par complex is recruited to the cell cortex and ultimately become tightly coupled to Par protein dynamics. Pulses are initially unoriented in interphase but are rapidly directed towards the apical pole in early mitosis, shortly before the Par protein aPKC accumulates on the cortex. The movements of cortical aPKC that lead to its polarization are precisely correlated with cortical actin pulses and F-actin disruption coincides with immediate loss of movement followed by depolarization. We find that myosin II is a component of the cortical pulses, suggesting that actomyosin pulsatile contractions initiate and maintain apical Par polarity during the neuroblast polarity cycle.

Introduction

The Par complex polarizes animal cells by excluding specific cortical factors from the Par cortical domain (Lang and Munro, 2017; Venkei and Yamashita, 2018). In *Drosophila* neuroblasts, for example, the Par domain forms at the apical cortex during mitosis where it prevents the spread of cortical neuronal fate determinants, effectively restricting them to the basal cortex. The resulting cortical domains are bisected by the cleavage furrow segregating the neuronal fate determinants into the basal daughter cell where they promote differentiation (Homem and Knoblich, 2012). It was recently discovered that apical Par polarization in the neuroblast is a multistep process in which the complex is initially targeted to the apical hemisphere early in mitosis where it forms a discontinuous meshwork (Kono et al., 2019; Oon and Prehoda, 2019). Cortical Par proteins then move along the cortex towards the apical pole, ultimately leading to formation of an apical cap that is maintained until shortly after anaphase onset (Oon and Prehoda, 2019). Here we examine how the cortical movements that initiate and potentially maintain neuroblast Par polarity are generated.

An intact actin cytoskeleton is known to be required for the movements that polarize Par proteins to the neuroblast apical cortex, but its role in the process has been unclear. Depolymerization of F-actin causes apical aPKC to spread to the basal cortex (Hannaford et al., 2018; Oon and Prehoda, 2019), prevents aPKC coalescence, and induces disassembly of the apical aPKC cap (Oon and Prehoda, 2019), suggesting that actin filaments are important for both apical polarity initiation and its maintenance. How the actin cytoskeleton participates

33 in polarizing the Par complex in neuroblasts has been unclear, but actomyosin plays a central
34 role in generating the anterior Par cortical domain in the *C. elegans* zygote. Pulsatile
35 contractions oriented towards the anterior pole transport the Par complex from an evenly
36 distributed state (Illukkumbura et al., 2019; Lang and Munro, 2017). Bulk transport is mediated
37 by advective flows generated by highly dynamic, transient actomyosin accumulations on the
38 cell cortex (Goehring et al., 2011). While pulsatile movements of actomyosin drive formation of
39 the Par domain in the worm zygote, and F-actin is required for apical Par polarity in the
40 neuroblast, no pulsatile contractions of actomyosin have been observed during the neuroblast
41 polarization process, despite extensive examination (Barros et al., 2003; Cabernard et al.,
42 2010; Connell et al., 2011; Koe et al., 2018; Roth et al., 2015; Roubinet et al., 2017; Tsankova
43 et al., 2017). Instead, both F-actin and myosin II have been reported to be cytoplasmic or
44 uniformly cortical in interphase, and apically enriched at metaphase (Barros et al., 2003; Koe et
45 al., 2018; Tsankova et al., 2017), before undergoing cortical flows towards the cleavage furrow
46 that are important for cell size asymmetry (Cabernard et al., 2010; Roubinet et al., 2017).

47 The current model for neuroblast actomyosin dynamics is primarily based on the analysis of
48 fixed cells or by imaging a small number of central optical sections in live imaging experiments
49 and we have recently found that rapid imaging of the full neuroblast volume can reveal
50 dynamic phases of protein movements (Oon and Prehoda, 2019). Here we use rapid full
51 volume neuroblast imaging to investigate whether pulsatile movements of cortical actomyosin
52 occur during early mitosis when the Par complex becomes polarized to the apical cortex.

53 **Results and Discussion**

54 **Pulsatile dynamics of cortical actin during neuroblast asymmetric divisions**

55 To gain insight into how actin participates in the neuroblast polarity cycle, we imaged larval
56 brain neuroblasts expressing an mRuby fusion of the actin sensor LifeAct (mRuby-LA) using
57 spinning disk confocal microscopy. The localization of this sensor in neuroblasts has been
58 reported (Abeysundara et al., 2018; Roubinet et al., 2017), but only during late mitosis. To
59 follow cortical actin dynamics across full asymmetric division cycles, we collected optical
60 sections through the entire neuroblast volume (~40 0.5 μm sections) at 10 second intervals
61 beginning in interphase and through at least one mitosis (Figure 1-figure supplement 1).
62 Acquiring full cell volume optical sections at this frequency required careful optimization to
63 prevent photobleaching while maintaining sufficient signal levels. Maximum intensity
64 projections constructed from these data revealed localized actin enrichments on the cortex,

65 some of which were highly dynamic (Figure 1 and Video 1). We observed four discrete phases
66 of cortical actin dynamics during neuroblast asymmetric divisions that we describe in detail
67 below.

68 The interphase neuroblast cortex was a mixture of patches of concentrated actin, highly
69 dynamic pulsatile waves that traveled across the entire width of the cell, and areas with little to
70 no detectable actin (Figure 1 and Video 1). Pulsatile movements consisted of the appearance
71 of actin on a localized area and moved rapidly across the cortex for approximately one minute
72 before disappearing (Figure 1A,E). Concentrated actin patches were relatively static, but
73 sometimes changed size over the course of several minutes but were mostly unaffected by the
74 pulsatile waves that occasionally passed over them. Pulses were sporadic in early interphase
75 but became more regular near mitosis, with a new pulse appearing immediately following the
76 completion of the prior one (Figure 1E and Video 1). The direction of the pulses during
77 interphase was highly variable, but often along the cell's equator (i.e. orthogonal to the
78 polarity/division axis). In general, actin in the interphase cortex was highly discontinuous and
79 included large areas with little to no detectable actin in addition to the patches and dynamic
80 pulses described above. Interphase pulses were correlated with cellular scale morphological
81 deformations in which these areas of low actin signal became distorted away from the cell
82 center while the cortex containing the actin pulse was compressed towards the center of the
83 cell (Figure 1D and Video 1).

84 A clear transition in the neuroblast cortex occurred several minutes before nuclear envelope
85 breakdown in which pulsatile movements shifted towards the apical pole and actin
86 accumulated at cortical regions with minimal actin in interphase (Figure 1B-E and Video 1). The
87 seemingly randomly oriented interphase pulses gave way to a highly regular progression of
88 apically-directed ones that traveled from the basal pole towards the apical pole (i.e. along the
89 polarity division axis). Pulses remained apically-directed until ceasing near the onset of
90 anaphase, leading to the apical actin enrichment that has been described previously (Barros et
91 al., 2003; Tsankova et al., 2017). Additionally, while the interphase cortex had areas with very
92 little actin, actin was more evenly-distributed following the transition (Figure 1D and Video 1).
93 Another rapid transition occurred shortly after anaphase onset, in which the apically-directed
94 cortical actin movements reversed direction such that the F-actin that had accumulated in the
95 apical hemisphere began to move basally towards the emerging cleavage furrow (Roubinet et
96 al., 2017).

97 **Apically directed actin pulses polarize aPKC**

98 Previously we showed that Par polarity proteins undergo complex cortical dynamics during
99 neuroblast asymmetric cell division, and that Par cortical movements require an intact actin
100 cytoskeleton (Oon and Prehoda, 2019). Examination of the cortical actin cytoskeleton revealed
101 that it also highly dynamic (Figure 1 and Video 1), with key transitions in cortical movements at
102 points in the cell cycle that are similar to those that occur in the protein polarity cycle. We
103 determined the extent to which cortical actin and aPKC dynamics are correlated by
104 simultaneously imaging GFP-aPKC expressed from its endogenous promoter with mRuby-
105 Lifeact (Figure 2 and Video 2). We observed aPKC targeting to the apical membrane beginning
106 approximately ten minutes before NEB, when small foci start to appear. The cortical pulses of
107 actin that passed over these aPKC enrichments had no noticeable effect on them, suggesting
108 that interphase cortical actin dynamics are not coupled to aPKC movement. Near NEB (e.g.
109 0:30 in Video 2), the continued accumulation of aPKC lead to a diffusely scattered distribution
110 over the apical hemisphere when the transition in actin cortical dynamics began. Continued
111 accumulation led to a discontinuous distribution of aPKC in the apical hemisphere near NEB
112 (e.g. -2:30 in Video 2). At this point, cortical actin pulses transitioned to the apically-directed
113 phase. While interphase pulses had no apparent effect on cortical aPKC, aPKC began moving
114 towards the apical pole when the apically-directed pulses began, and these movements
115 continued until it became fully polarized (3:50 in Video 2). Cortical actin pulses continued with
116 no apparent change in the polarized aPKC apical cap for several minutes (until approximately
117 7:20 in Video 2) when cortical actin and aPKC began simultaneously moving basally, toward
118 the emerging cleavage furrow. Thus, cortical aPKC does not appear to be coupled to
119 interphase actin pulses, but its movements are highly correlated with the apically-directed
120 pulses that begin in early mitosis. Cortical actin pulses continue even after aPKC is fully
121 polarized and both actin and aPKC simultaneously begin moving basally towards the cleavage
122 furrow in anaphase.

123 Simultaneous imaging of aPKC and actin allowed us to examine precisely when disruption of
124 the actin cytoskeleton influences aPKC dynamics (Figure 3 and Figure 3-videos 1-3). We
125 introduced the actin depolymerizing drug Latrunculin A (LatA) at different phases of the cell
126 cycle and examined how the movement of cortical aPKC was influenced as the cortical actin
127 signal dissipated. We previously found that the actin cytoskeleton is required for the apically-
128 directed polarizing movements of aPKC. Here we find that when cortical actin signal dissipates

129 immediately before the targeting phase (Figure 3A,A' and Figure 3-video 1), aPKC is recruited
130 to the apical cortex but rapidly depolarizes. When actin dissipates after aPKC is targeted to the
131 apical cortex and has begun coalescing at the apical pole (Figure 3B,B' and Figure 3-video 2),
132 aPKC movement ceases immediately following the loss of cortical actin and the remaining
133 aPKC diffuses into the basal cortex and becomes depolarized as observed previously. Finally,
134 when cortical actin dissipates after the aPKC apical cap is formed, we see aPKC begins
135 diffusing away from the apical immediately following the disappearance of the cortical actin
136 signal (Figure 3C,C' and Figure 3-video 3). Thus, cortical actin and aPKC dynamics are highly
137 correlated, and cortical aPKC movement is dependent on cortical actin, ceasing immediately
138 following the loss of cortical actin.

139 **Myosin II is a component of neuroblast cortical pulses**

140 We observed morphological changes in interphase cells (Figure 1D and Video 1), and cortical
141 aPKC movements that were correlated with cortical actin dynamics in early mitosis (Figure 2
142 and Video 2). These phenomena are consistent with force generation by the cortical actin
143 pulses. While actin can generate force through polymerization, contractile forces are generated
144 when it is paired with myosin II, and cortical pulsatile contractions of actomyosin have been
145 observed in other systems (Michaux et al., 2018; Munro et al., 2004). Although there are
146 numerous reports of myosin II dynamics in neuroblasts (Barros et al., 2003; Koe et al., 2018;
147 Tsankova et al., 2017), no cortical pulses have been described and its localization has been
148 described as uniformly cortical or cytoplasmic in interphase and before metaphase in mitosis.
149 We used rapid imaging of the full cell volume, simultaneously following a GFP fusion of the
150 myosin II regulatory light chain Spaghetti squash (GFP-Sqh) with mRuby-Lifeact, to determine
151 if myosin II is part of the cortical actin pulses we observed. We found that myosin II is a
152 component of every phase of the actin pulses (Figure 4 and Video 3), including the apically-
153 directed pulses that polarize aPKC. Interestingly, however, while myosin II localized with actin
154 and had very similar dynamics, the localization between the two was not absolute and there
155 were often large cortical regions where the two did not colocalize in addition to the region
156 where they overlapped (Figure 4 and Video 3). This is similar to the localization of the two
157 proteins in the polarizing worm zygote (Michaux et al., 2018; Reymann et al., 2016). We also
158 noticed that myosin II pulses were less persistent than their actin counterparts during the
159 apically-directed phase of dynamics (Figure 4C). Thus, while there are some differences in the

160 dynamics of the two proteins, myosin II is a component of interphase and early mitotic
161 neuroblast cortical pulses.

162 **A role for actomyosin pulsatile contractions in the initiation and maintenance of apical**
163 **Par polarity in neuroblasts**

164 Our results reveal previously unrecognized phases of pulsatile contractions during cycles of
165 neuroblast asymmetric divisions. During interphase, transient cortical patches of actomyosin
166 undergo highly dynamic movements in which they rapidly traverse the cell cortex,
167 predominantly along the cell's equator, before dissipating and a new cycle begins (Figure 1A).
168 Shortly after mitotic entry the pulsatile movements reorient to align with the polarity axis.
169 Importantly, the transition between these phases occurs shortly before the establishment of
170 apical Par polarity, when discrete cortical patches of aPKC undergo coordinated movements
171 towards the apical pole to form an apical cap. Pulsatile movements continue past metaphase
172 when apical cap assembly is completed, suggesting that they may also be involved in cap
173 maintenance.

174 The actomyosin dynamics we have uncovered provide a framework for understanding how
175 actomyosin participates in neuroblast apical polarity. First, apically directed pulsatile
176 movements of actomyosin are consistent with the requirement for F-actin in the cortical flows
177 that lead to coalescence of discrete aPKC patches (Figure 3) (Oon and Prehoda, 2019).
178 Furthermore, the continuation of myosin II pulsatile movements after cap assembly is
179 completed implies that they are also important for polarity maintenance (Figure 3). A role for
180 actomyosin in cap maintenance would explain why the cap becomes dissociated when F-actin
181 is depolymerized shortly after cap assembly (Oon and Prehoda, 2019). How might myosin II
182 pulsatile contractions lead to the cortical flows we have observed during the polarization of the
183 neuroblast apical cortex? Studies of worm zygote Par polarity provide a possible explanation.
184 In this system, pulsatile contractions generate bulk cortical flows (i.e. advection) that lead to
185 non-specific transport of cortically localized components (Goehring et al., 2011; Illukkumbura
186 et al., 2019). Whether the cortical flows that occur during apical polarization of the neuroblast
187 are also driven by advection will require further study.

188 **Materials and Methods**

189

190 **Key Resources Table**

Reagent type (species) or resource	Designation	Source or reference	Identifiers	Additional information
Genetic reagent (*Drosophila melanogaster*)	LifeAct-Ruby	Bloomington Drosophila Stock Center	BDSC:35545; FLYB:FBti0143328; RRID:BDSC_35545	FlyBase symbol: P{UAS-Lifeact-Ruby}VIE-19A
Genetic reagent (*D. melanogaster*)	insc-Gal4	Chris Doe Lab; Bloomington Drosophila Stock Center	BDSC:8751; FLYB:FBti0148948; RRID:BDSC_8751	FlyBase symbol: P{GawB}insc^{Mz1407}
Genetic reagent (*D. melanogaster*)	aPKC-GFP	François Schweisguth Lab; Besson et al., 2015		BAC encoded aPKC-GFP
Genetic reagent (*D. melanogaster*)	wor-Gal4	Chris Doe Lab; Bloomington Drosophila Stock Center	BDSC:56553; FLYB:FBti0161165; RRID:BDSC_56553	FlyBase symbol: P{wor.GAL4.A}2
Genetic reagent (*D. melanogaster*)	Sqh-GFP	Royou et al., 2002		Expressed by natural *sqh* promoter

191

192 *Fly strains and genetics*

193 UAS-LifeAct-Ruby (Bloomington stock 35545), BAC-encoded aPKC-GFP (Besson et al., 2015)
194 and Sqh-GFP (Royou et al., 2002) transgenes were used to assess F-actin, aPKC and myosin II
195 dynamics, respectively. Expression of LifeAct was specifically driven in nerve cells upon
196 crossing UAS-LifeAct-Ruby to insc-Gal4 (1407-Gal4, Bloomington stock 8751) or to wor-Gal4
197 (Bloomington stock 56553). The following genotypes were examined through dual channel live
198 imaging: BAC-aPKC-GFP/Y ; insc-Gal4, UAS-LifeAct-Ruby/+ and ; worGal4, Sqh-GFP, UAS-
199 LifeAct-Ruby/+ ;.

200 *Live imaging*

201 Third instar larvae were incubated in 30˚C overnight (~12 hours) prior to imaging and were
202 dissected to isolate the brain lobes and ventral nerve cord, which were placed in Schneider's
203 Insect media (SIM). Larval brain explants were placed in lysine-coated 35 mm cover slip dishes
204 (WPI) containing modified minimal hemolymph-like solution (HL3.1). Explants were imaged on a
205 Nikon Ti2 microscope equipped with a Yokogawa CSU-W1 spinning disk that was configured
206 to two identical Photometrics Prime BSI Scientific CMOS cameras for simultaneous dual
207 channel live imaging. Using the 1.2 NA Plan Apo VC water immersion objective, explants were

208 magnified at 60x for visualization. Explants expressing LifeAct-Ruby, aPKC-GFP and Sqh-GFP
209 were illuminated with 488 nm and 561 nm laser light throughout approximately 41 optical
210 sections with step size of 0.5 μm and time interval of 10 seconds.

211 *Image processing, analysis and visualization*
212 Movies were analyzed in ImageJ (using the FIJI package) and in Imaris (Bitplane). Neuroblasts
213 whose apical-basal polarity axis is positioned parallel to the imaging plane were cropped out to
214 generate representative images and movies. Cortical edge and central maximum intensity
215 projections (MIP) were derived from optical slices capturing the surface and center of the cell,
216 respectively. Cortical MIPs were also used to perform kymograph analysis, where the change
217 in localization profile of fluorescently-tagged fusion proteins within a 3 to 5 pixels wide region
218 was examined across time. To track cortical movements over the length of the apical-basal
219 axis, a vertical region parallel to the polarity axis was specified for the kymograph analysis.
220 Similarly, a horizontal line orthogonal to the polarity axis that is superimposing on the
221 presumptive equator was specified for examining equatorial motions. Optical sections
222 capturing the whole of the cell were assembled for 3D rendering and visualization in FIJI or
223 Imaris. These volumetric reconstructions were then used to determine the timing of cortical
224 motions characterized in this paper.

225 **Video Legends**
226 Video 1 Actin dynamics in a larval brain neuroblast.
227 The mRuby-Lifeact sensor expressed from the UAS promoter and *worniu-GAL4* (drives
228 expressing in neuroblasts and progeny) is shown with a maximum intensity projection of the
229 front hemisphere of the cell.

230 Video 2 Correlated dynamics of the Par protein aPKC and Actin in a larval brain neuroblast.
231 GFP-aPKC expressed from its endogenous promoter and the mRuby-Lifeact sensor expressed
232 from the UAS promoter and *worniu-GAL4* (drives expressing in neuroblasts and progeny) are
233 shown from simultaneously acquired optical sections with a maximum intensity projection of
234 the front hemisphere of the cell.

235 Figure 3-video 1 Correlated dynamics of the Par protein aPKC and Actin in a larval brain
236 neuroblast treated with Latrunculin A before mitosis.
237 GFP-aPKC expressed from its endogenous promoter and the mRuby-Lifeact sensor expressed

238 from the UAS promoter and *worniu-GAL4* (drives expressing in neuroblasts and progeny) are
239 shown from simultaneously acquired optical sections with a maximum intensity projection of
240 the front hemisphere of the cell. Lat A was added to the media surrounding the larval brain
241 explant at the indicated time.

242 Figure 3-video 2 Correlated dynamics of the Par protein aPKC and Actin in a larval brain
243 neuroblast treated with Latrunculin A during prophase.
244 GFP-aPKC expressed from its endogenous promoter and the mRuby-Lifeact sensor expressed
245 from the UAS promoter and *worniu-GAL4* (drives expressing in neuroblasts and progeny) are
246 shown from simultaneously acquired optical sections with a maximum intensity projection of
247 the front hemisphere of the cell. Lat A was added to the media surrounding the larval brain
248 explant at the indicated time.

249 Figure 3-video 3 Correlated dynamics of the Par protein aPKC and Actin in a larval brain
250 neuroblast treated with Latrunculin A during metaphase.
251 GFP-aPKC expressed from its endogenous promoter and the mRuby-Lifeact sensor expressed
252 from the UAS promoter and *worniu-GAL4* (drives expressing in neuroblasts and progeny) are
253 shown from simultaneously acquired optical sections with a maximum intensity projection of
254 the front hemisphere of the cell. Lat A was added to the media surrounding the larval brain
255 explant at the indicated time.

256 Video 3 Correlated dynamics of myosin II and Actin in a larval brain neuroblast.
257 GFP-Sqh (the myosin II regulatory light chain, Spaghetti Squash) expressed from its
258 endogenous promoter and the mRuby-Lifeact sensor expressed from the UAS promoter and
259 *worniu-GAL4* (drives expressing in neuroblasts and progeny) are shown from simultaneously
260 acquired optical sections with a maximum intensity projection of the front hemisphere of the
261 cell and the medial optical section. The neuroblast is highlighted by a dashed circle.

262

263

References

Abeysundara N, Simmonds AJ, Hughes SC. 2018. Moesin is involved in polarity maintenance and cortical remodeling during asymmetric cell division. *Mol Biol Cell* **29**:419–434. doi:10.1091/mbc.E17-05-0294

Barros CS, Phelps CB, Brand AH. 2003. Drosophila nonmuscle myosin II promotes the asymmetric segregation of cell fate determinants by cortical exclusion rather than active transport. *Dev Cell* **5**:829–840.

Besson C, Bernard F, Corson F, Rouault H, Reynaud E, Keder A, Mazouni K, Schweisguth F. 2015. Planar Cell Polarity Breaks the Symmetry of PAR Protein Distribution prior to Mitosis in Drosophila Sensory Organ Precursor Cells. *Curr Biol CB* **25**:1104–1110. doi:10.1016/j.cub.2015.02.073

Cabernard C, Prehoda KE, Doe CQ. 2010. A spindle-independent cleavage furrow positioning pathway. *Nature* **467**:91–94. doi:10.1038/nature09334

Connell M, Cabernard C, Ricketson D, Doe CQ, Prehoda KE. 2011. Asymmetric cortical extension shifts cleavage furrow position in Drosophila neuroblasts. *Mol Biol Cell* **22**:4220–4226. doi:10.1091/mbc.E11-02-0173

Goehring NW, Trong PK, Bois JS, Chowdhury D, Nicola EM, Hyman AA, Grill SW. 2011. Polarization of PAR proteins by advective triggering of a pattern-forming system. *Science* **334**:1137–1141. doi:10.1126/science.1208619

Hannaford MR, Ramat A, Loyer N, Januschke J. 2018. aPKC-mediated displacement and actomyosin-mediated retention polarize Miranda in Drosophila neuroblasts. *eLife* **7**. doi:10.7554/eLife.29939

Homem CCF, Knoblich JA. 2012. Drosophila neuroblasts: a model for stem cell biology **139**:4297–4310. doi:10.1242/dev.080515

Illukkumbura R, Bland T, Goehring NW. 2019. Patterning and polarization of cells by intracellular flows. *Curr Opin Cell Biol* **62**:123–134. doi:10.1016/j.ceb.2019.10.005

Koe CT, Tan YS, Lönnfors M, Hur SK, Low CSL, Zhang Y, Kanchanawong P, Bankaitis VA, Wang H. 2018. Vibrator and PI4KIIIα govern neuroblast polarity by anchoring non-muscle myosin II. *eLife* **7**. doi:10.7554/eLife.33555

Kono K, Yoshiura S, Fujita I, Okada Y, Shitamukai A, Shibata T, Matsuzaki F. 2019. Reconstruction of Par-dependent polarity in apolar cells reveals a dynamic process of cortical polarization. *eLife* **8**. doi:10.7554/eLife.45559

Lang CF, Munro E. 2017. The PAR proteins: from molecular circuits to dynamic self-stabilizing cell polarity. *Dev Camb Engl* **144**:3405–3416. doi:10.1242/dev.139063

Michaux JB, Robin FB, McFadden WM, Munro EM. 2018. Excitable RhoA dynamics drive pulsed contractions in the early C. elegans embryo. *J Cell Biol* **217**:4230–4252. doi:10.1083/jcb.201806161

Munro E, Nance J, Priess JR. 2004. Cortical flows powered by asymmetrical contraction transport PAR proteins to establish and maintain anterior-posterior polarity in the early C. elegans embryo. *Dev Cell* **7**:413–424. doi:10.1016/j.devcel.2004.08.001

Oon CH, Prehoda KE. 2019. Asymmetric recruitment and actin-dependent cortical flows drive the neuroblast polarity cycle. *eLife* **8**. doi:10.7554/eLife.45815

Reymann A-C, Staniscia F, Erzberger A, Salbreux G, Grill SW. 2016. Cortical flow aligns actin filaments to form a furrow. *eLife* **5**. doi:10.7554/eLife.17807

Roth M, Roubinet C, Iffländer N, Ferrand A, Cabernard C. 2015. Asymmetrically dividing Drosophila neuroblasts utilize two spatially and temporally independent cytokinesis pathways. *Nat Commun* **6**:6551. doi:10.1038/ncomms7551

311 Roubinet C, Tsankova A, Pham TT, Monnard A, Caussinus E, Affolter M, Cabernard C. 2017.
312 Spatio-temporally separated cortical flows and spindle geometry establish physical
313 asymmetry in fly neural stem cells. *Nat Commun* **8**:1383. doi:10.1038/s41467-017-
314 01391-w
315 Royou A, Sullivan W, Karess R. 2002. Cortical recruitment of nonmuscle myosin II in early
316 syncytial Drosophila embryos: its role in nuclear axial expansion and its regulation by
317 Cdc2 activity. *J Cell Biol* **158**:127–137. doi:10.1083/jcb.200203148
318 Tsankova A, Pham TT, Garcia DS, Otte F, Cabernard C. 2017. Cell Polarity Regulates Biased
319 Myosin Activity and Dynamics during Asymmetric Cell Division via Drosophila Rho
320 Kinase and Protein Kinase N. *Dev Cell* **42**:143-155.e5. doi:10.1016/j.devcel.2017.06.012
321 Venkei ZG, Yamashita YM. 2018. Emerging mechanisms of asymmetric stem cell division. *J*
322 *Cell Biol*. doi:10.1083/jcb.201807037
323

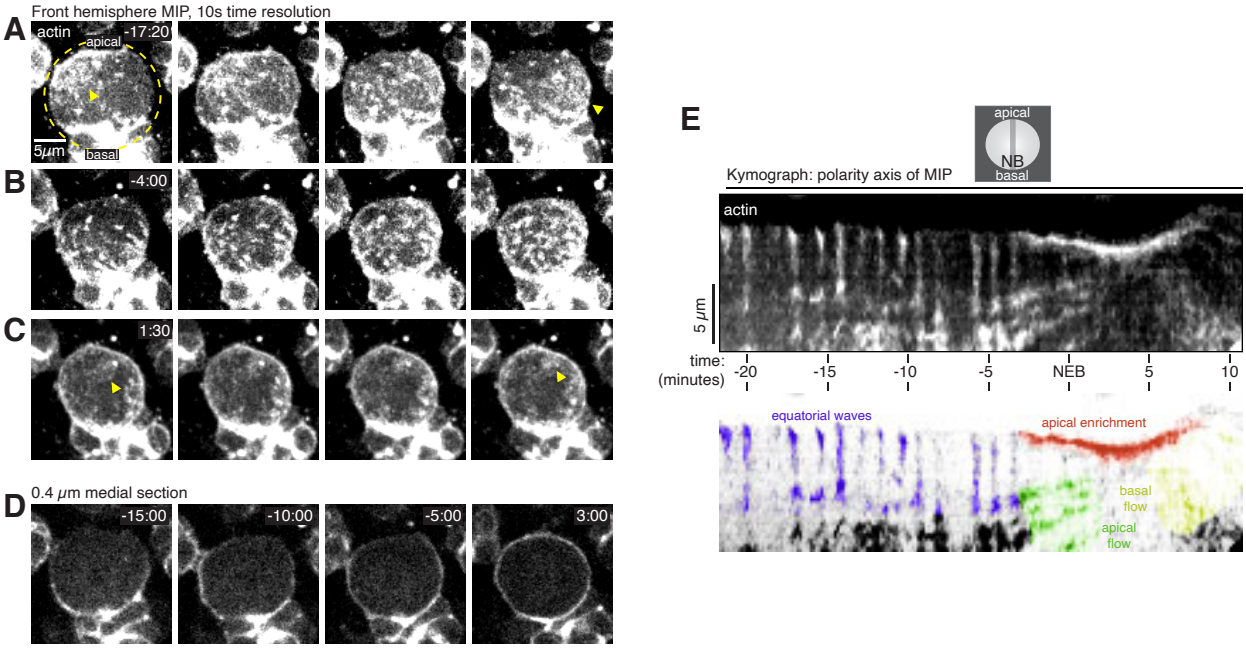

Figure 1 Cortical F-actin dynamics in asymmetrically dividing *Drosophila* larval brain neuroblasts. (**A**) Selected frames from Video 1 showing cortical actin pulses during interphase. mRuby-LifeAct expressed via insc-GAL4/UAS (”actin”) is shown via a maximum intensity projection (MIP) constructed from optical sections through the front hemisphere of the cell.The outline of the neuroblast is shown by a dashed yellow circle. Arrowhead marks an example cortical actin patch. Time (mm:ss) is relative to nuclear envelope breakdown. (**B**) Selected frames from Video 1 as in panel A showing cortical actin moving apically. (**C**) Selected frames from Video 1 as in panel A showing cortical actin enriched on the apical cortex. (**D**) Selected frames from Video 1 showing how actin becomes cortically enriched near NEB. Medial cross sections show the cortical actin signal is relatively discontinuous until NEB approaches. (**E**) Kymograph constructed from frames of Video 1 using sections along the apical-basal axis as indicated. A legend for the features in the kymograph is included below.

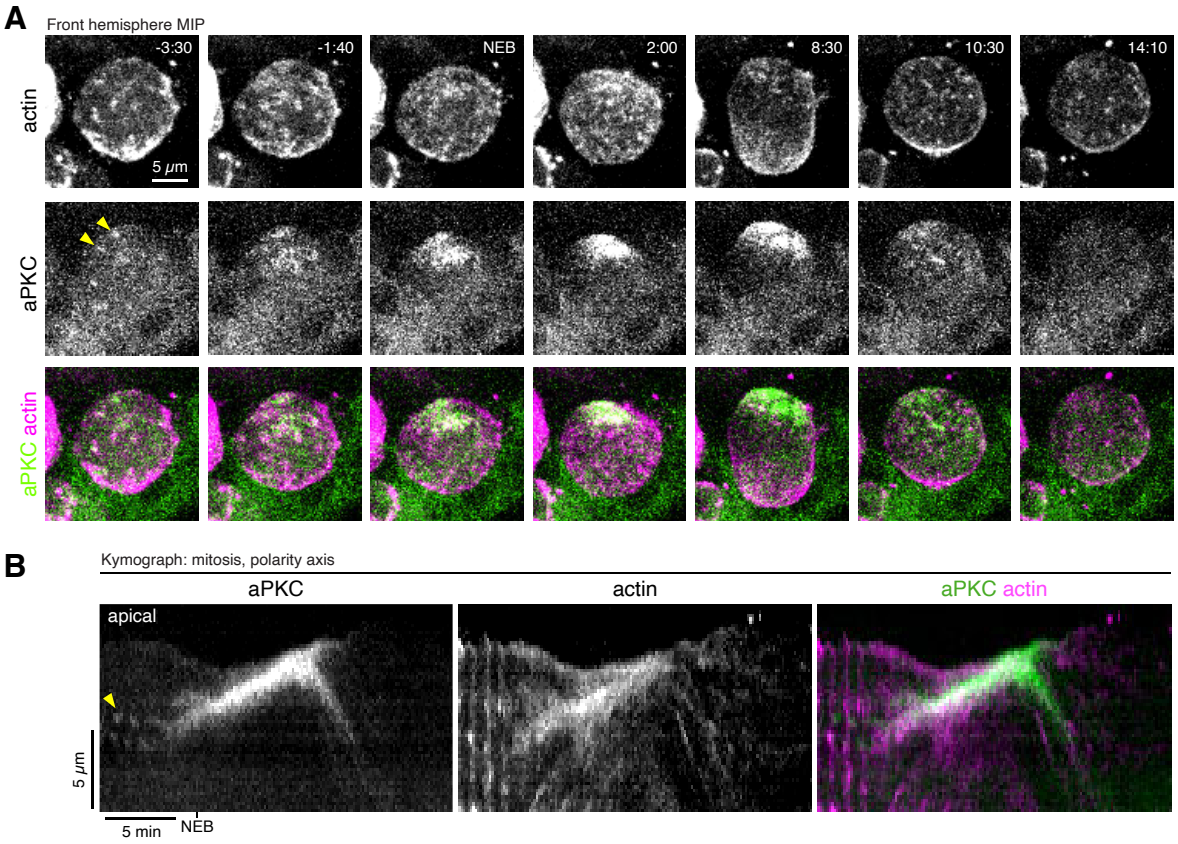

Figure 2 Coordinated actin and aPKC dynamics during the neuroblast polarity cycle. (**A**) Selected frames from Video 2 showing the correlated dynamics of aPKC and actin during polarization and depolarization. aPKC-GFP expressed from its endogenous promoter (”aPKC”) and mRuby-LifeAct expressed via insc-GAL4/UAS (”actin”) are shown via a maximum intensity projection (MIP) constructed from optical sections through the front hemisphere of the cell. (**B**) Kymograph made from a segment along the apical-basal axis of the neuroblast in Video 2 showing the correlated dynamics of aPKC and actin.

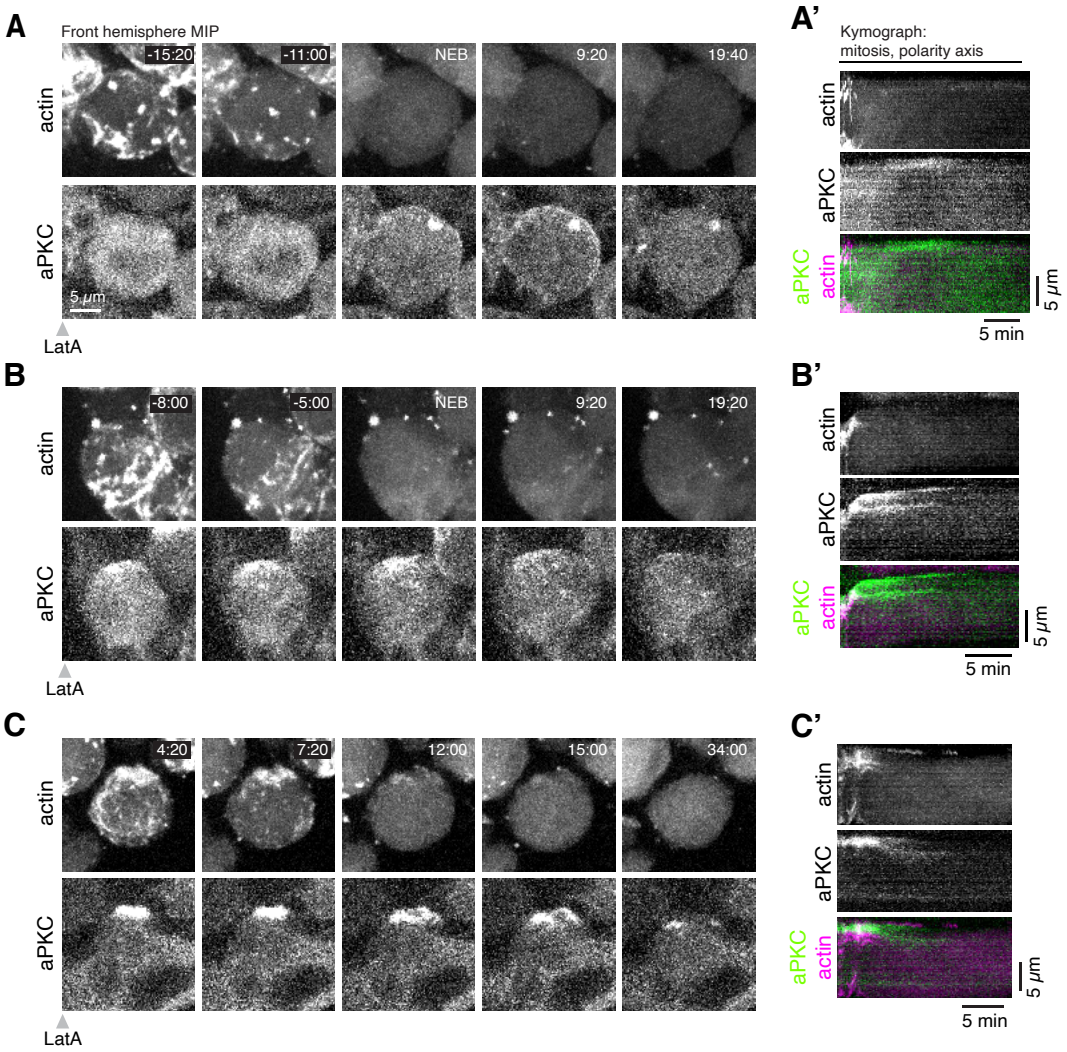

Figure 3 Effect of LatA on actin and aPKC dynamics. (**A-C**) Selected frames from Figure 3-videos 1-3 showing how loss of cortical actin before mitosis (A), at NEB (B), and during metaphase (C) influences aPKC dynamics. aPKC-GFP expressed from its endogenous promoter ("aPKC") and mRuby-LifeAct expressed via insc-GAL4/UAS ("actin") are shown via a maximum intensity projection (MIP) constructed from optical sections through the front hemisphere of the cell. The scale bar applies to all panels in A-C. (**A'-C'**) Kymographs for A' and C' are made from Figure 3-videos 1 and 3 using a section of each frame along the apical-basal axis. The kymograph in B' is made from a different cell than shown in (B) and FIgure 3-video 2.

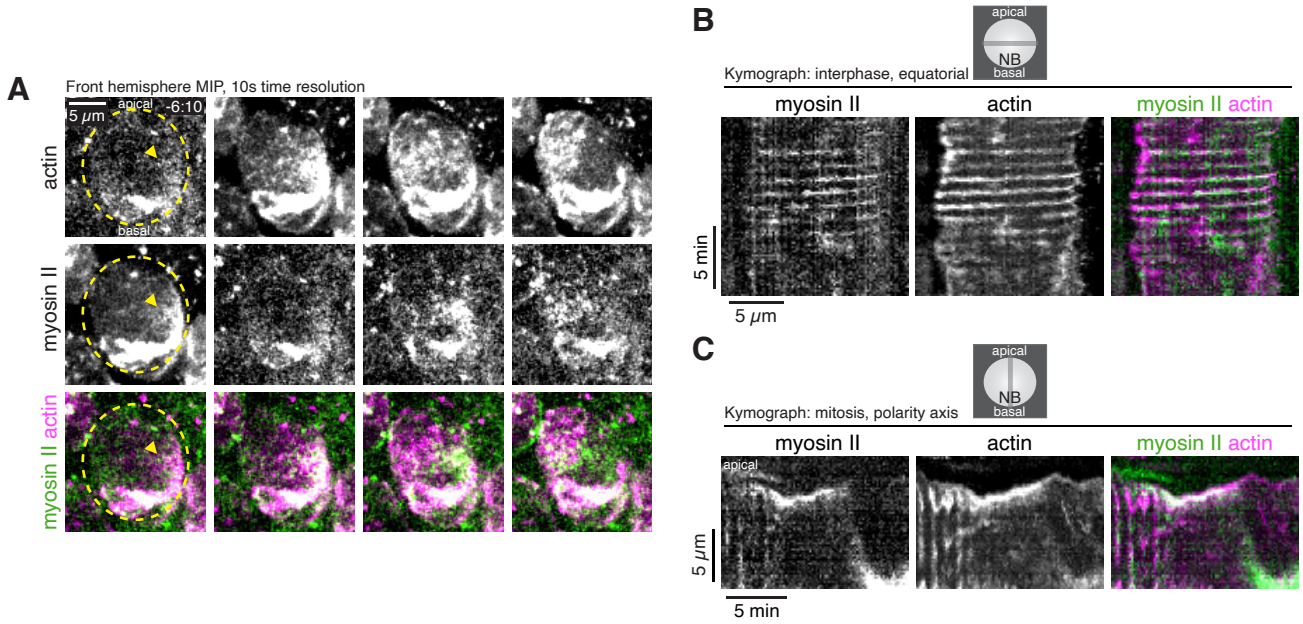

Figure 4 Dynamics of cortical actomyosin in asymmetrically dividing *Drosophila* larval brain neuroblasts. (**A**) Selected frames from Video 3 showing cortical actomyosin traveling across the equatorial face of the cell. GFP-Sqh expressed from its endogenous promoter (”Myosin II”) and mRuby-LifeAct expressed via worniu-GAL4/UAS (”actin”) are shown via a maximum intensity projection (MIP) constructed from optical sections through the front hemisphere of the cell.The outline of the neuroblast is shown by a dashed yellow line and arrowheads indicate the starting position of the cortical patches. Time is relative to nuclear envelope breakdown. (**B**) Kymograph constructed from frames of Video 3 during interphase using sections through the equatorial region of the cell as indicated. (**C**) Kymograph constructed from frames of Video 3 during mitosis using sections along the polarity axis of the cell as indicated.

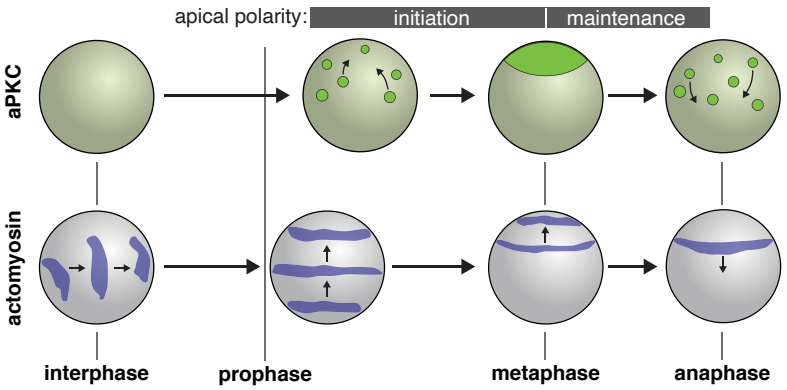

Figure 5 Model for role of actomyosin in neuroblast Par polarity. During interphase when aPKC is cytoplasmic, myosin II pulsatile contractions are predominantly equatorial. During apical polarity initiation in prophase and shortly before when discrete aPKC cortical patches begin to undergo coordinated movements towards the apical pole, myosin II pulsatile contractions reorient towards the apical cortex. Contractions are initially over a large surface area but become concentrated to the apical cortex as aPKC apical cap assembly is completed and the maintenance phase begins. At anaphase apical myosin II is cleared as it flows towards the cleavage furrow while the aPKC cap is disassembled.

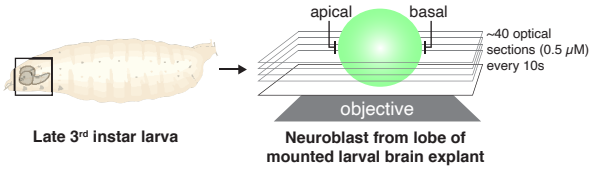

Figure 1 - figure supplement 1 Imaging and analysis scheme for rapid, full volume imaging of Drosophila neuroblasts from larval brain explants. Larval brains from 3rd instar larvae were mounted and imaged along the neuroblast polarity axis (”apical” and “basal”). Optical sections across the full cell volume were acquired every 7-10 seconds and used to construct maximum intensity projections.